

Supplementary (S) Tables and Figures

Table S1 Summary of Gaseous Oxidized Mercury Measurement Techniques

Reference	Sample Collection	Analyte Recovery	Detector	Form of Hg(II) Measured	Sampling Time	Max. GOM Measured ^a	Detection limit
					(h)	(pg m ⁻³)	
Tong et al., 1999	None	None	PFFS	HgBr ₂	0.003	8 × 10 ¹¹	1.5 × 10 ⁸
Stratton et al., 2001	HCl/NaCl Mist Chamber	Chemical Reduction	CV-AFS	Total GOM	1	3000	4
Landis et al., 2002	KCl Denuder	Pyrolysis	CV-AFS	Total GOM	1 – 12	1500	0.5 – 6
Olson et al., 2002	MnO ₂ Sorbent	Solvent Trapping + Injection	GC-MS	HgNO ₃ ; HgCl ₂	1	NR	NR
Lyman et al., 2010	Cation Exchange Membrane	Chemical Reduction	CV-AFS	Total GOM	336	60	2 – 7
Lyman and Jaffe, 2012	None	Pyrolysis	CV-AFS	GOM+ Hg _(P) ^b	0.04	1100	70
Huang et al., 2013	Nylon Membrane	Thermal Desorption + Pyrolysis	CV-AFS	HgO; HgCl ₂ ; HgBr ₂ ^c	8	50	NR
Huang et al., 2013	Cation Exchange Membrane	Chemical Reduction	CV-AFS	Total GOM	8	3000	3
This Study	Particle-based Sorbent Trap	Thermal Desorption	APCI-MS	HgCl ₂ ; HgBr ₂	24	480	4;7

PFFS – Laser Photofragment Fluorescence Spectroscopy; CV-AFS – Cold Vapor Atomic Fluorescence Spectroscopy; APCI-MS – Atmospheric Pressure Chemical Ionization Mass Spectrometry; GC-MS – Gas Chromatography Mass Spectrometry

a – Reported values not necessarily upper limits for techniques

b – Inferred from total mercury and elemental mercury measurements

c – Identified from thermal desorption curves

Table S2 A Comparison of HgX₂ Trapping and Recovery with Differing Trap Composition

Trap Composition	HgX ₂ Standard Used	Exposure Time (sec)	Desorption Temperature (°C)	Peak Height m/z=291 (cts)	Peak Height m/z=381 (cts)	
Shredded Teflon	HgCl ₂	5	150	2.6 × 10 ³	—	
				3.3 × 10 ³	—	
				1.5 × 10 ³	—	
	8:1 HgCl ₂ :HgBr ₂	60	200	9.4 × 10 ³	6.6 × 10 ³	
Polysulfide S4	HgCl ₂	60	150	5	4 × 10 ²	—
				10	4 × 10 ²	—
			200	1.4 × 10 ⁴	—	
				2.0 × 10 ⁴	—	
			8:1 HgCl ₂ :HgBr ₂	4.9 × 10 ³	3.6 × 10 ³	
			Magnetite		50	not detected
Silver	HgCl ₂	60	150	5 × 10 ²	—	
			200	5.8 × 10 ³	—	
				6.0 × 10 ³	—	
			325	5.2 × 10 ³	—	
				1.6 × 10 ³	—	
			8:1 HgCl ₂ :HgBr ₂	1.5 × 10 ⁴	1.1 × 10 ⁴	
	7.6 × 10 ³	4.8 × 10 ³				
All Teflon ^a	HgCl ₂		150	1.2 × 10 ³	—	
CoCl	8:1 HgCl ₂ :HgBr ₂	60	200	1.6 × 10 ³	—	
				8.8 × 10 ³	7.1 × 10 ³	
Glass Wool	HgCl ₂			9 × 10 ²	—	

Gray Font – Non-identification of HgX₂ due to contaminants; Value given is an upper limit to target ion peak height.

a – Shredded Teflon trap capped with Teflon frits in a 6.3 mm PFA tube

Table S3 A multi-point calibration of preconcentration + APCI analysis of HgX₂

HgX ₂	APCI gas	n	Mass Range (ng)	Sensitivity (cts pg ⁻¹)	R ²	Method Detection Limit (pg)
HgCl ₂	10% IB in N ₂	12	0.05 – 1.6	6 × 10 ¹	0.95	14
HgBr ₂	10% IB in N ₂	13	0.09 – 3.6	12	0.96	4 × 10 ¹
HgCl ₂	0.5% SF ₆ in IB	11	0.3 – 1.0	1.4 × 10 ²	0.78	6
HgBr ₂	0.5% SF ₆ in IB	14	0.6 – 18	5 × 10 ¹	0.99	17

Table S4 Urban/indoor air measurements in Montreal, Canada 2013-2014

Year	Start Date	Stop Date	Trap	HgCl ₂	HgBr ₂
				pg m ⁻³	
Burnside Hall, McGill University Campus, Montreal Canada (urban, ~50 m above ground level)					
2013	224.67	225.67	PS	5×10^1	<11
			Tef A	1×10^2	$<6 \times 10^1$ *
			GB	7×10^1	19
	228.67	231.67	Tef A	8×10^1	9×10^1
			TL	<17*	12
			Tef B + PS	<29*	<24*
	242.67	245.67	TL	<12*	<11
			Tef B + PS	<6*	<11
	273.67	274.67	Tef A	4×10^1	3×10^1
			TL	$<4 \times 10^1$ *	<24 *
T			29	9×10^1	
2014	14.67	15.67	PS	<4	<11
			Tef A	7	<11
			Tef B	<6 *	<11
Memorial Pool, McGill University Campus, Montreal Canada (indoor)					
2014	27.92	28.42	PS	$<6 \times 10^1$ *	<19 *
			Tef A	8×10^1	$<6 \times 10^1$ *
			CoCl	$<2 \times 10^2$ *	<11
	34.92	35.42	PS	27	<26 *
			Tef A	5×10^1	29
	64.92	65.42	PS	16	5×10^1
			Tef A	8×10^1	$<1.4 \times 10^2$ *
	65.92	66.42	PS	<4	<11
			Tef A	4×10^1	$<1.2 \times 10^2$ *

PS – Polysulfide-coated copper/iron nanoparticles, GB – glass beads, Tef – shredded Teflon, TL – shredded Teflon in GC liner, T – shredded Teflon in Teflon tubing (all Teflon), CoCl – cobalt chloride crystals, Tef + PS – Teflon trap with PS precolumn.

* - Contaminants present based on qualifier-target ion ratios. Concentration is an upper limit to possible HgX₂ concentration.

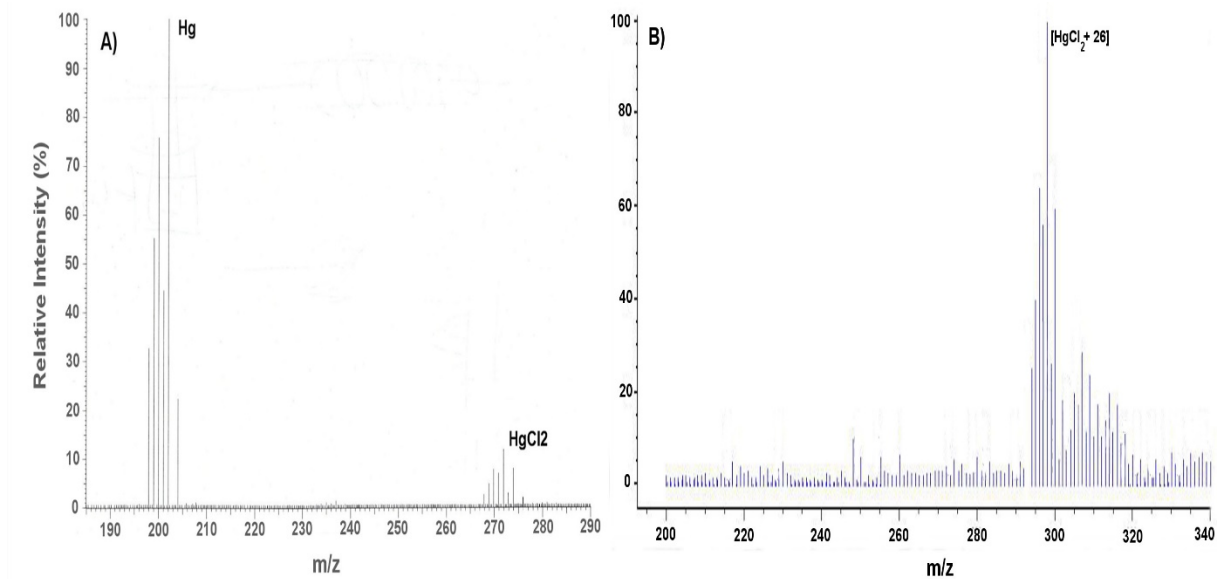


Figure S1 A comparison of EI-MS analysis of $\sim 1 \mu\text{mol HgCl}_{2(s)}$ (a) and APCI-MS analysis of $\sim 1 \text{ pmol HgCl}_{2(g)}$ using 10% isobutane in nitrogen as a CI gas (b). The EI-MS spectrum shows significant fragmentation (i.e. loss of chemical identity), while the APCI-MS preserves the mercury halide as an ion complex with an isobutane fragment ($m/z=26$) that is readily interpretable as originating from HgCl_2 .

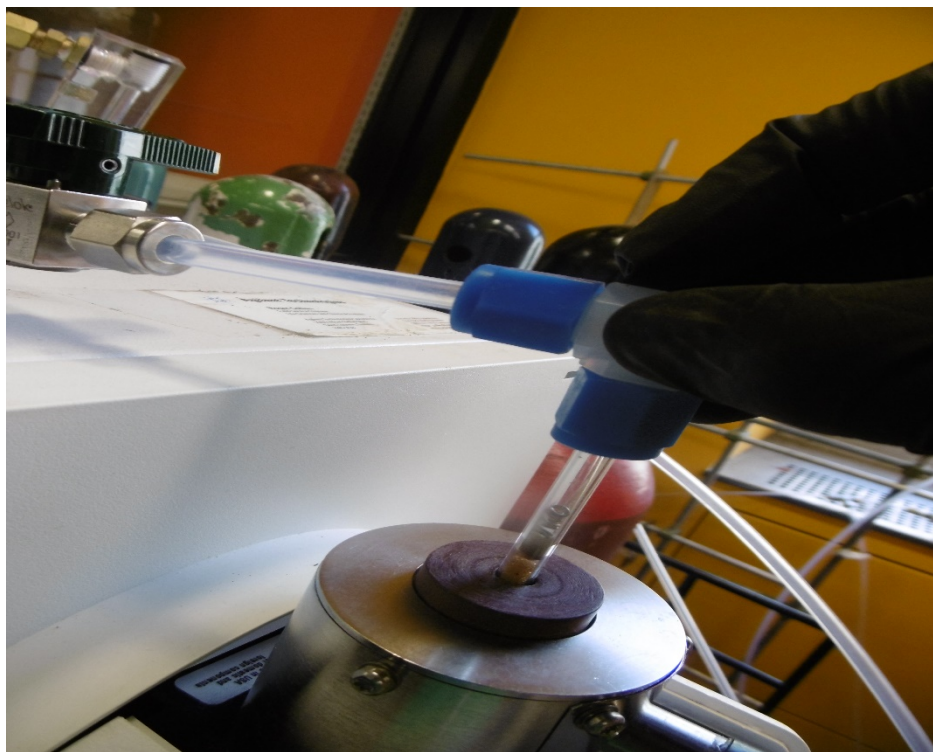


Figure S2 Photograph showing sorbent trap being inserted into modified APCI inlet while connected to the CI gas line with no gas flow.

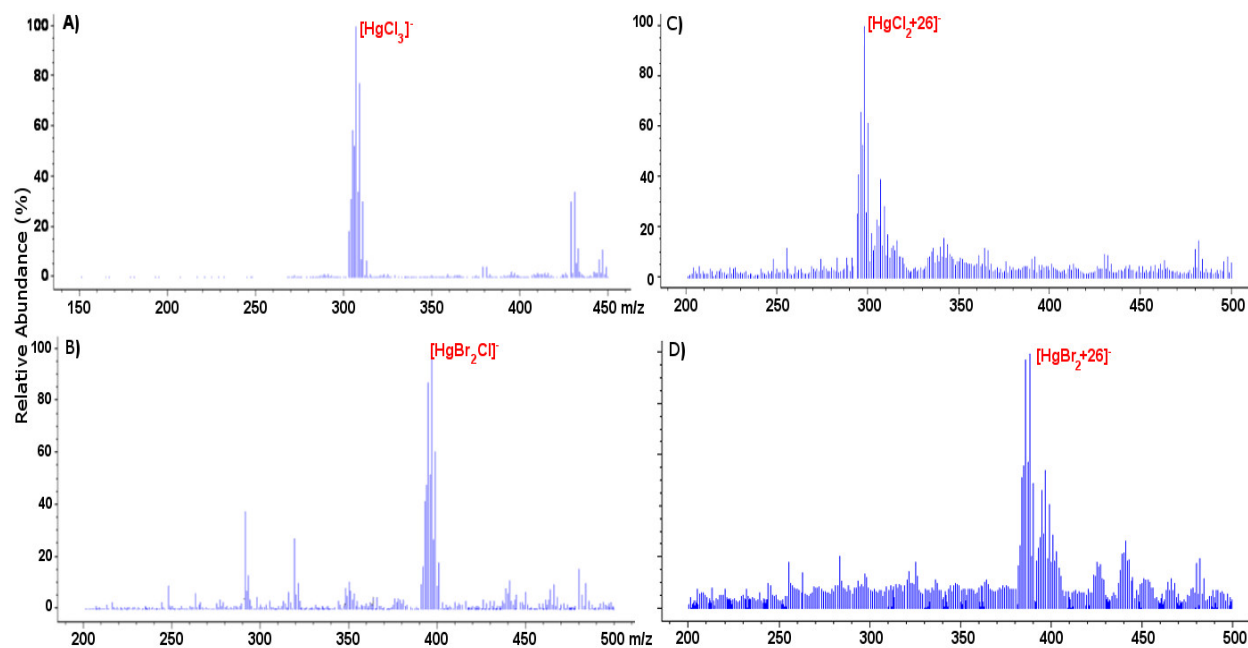


Figure S3 APCI scans of HgCl₂ and HgBr₂ packed standards with nitrogen (a,b) and 10% isobutane in nitrogen (c,d) as CI gas. HgX₂ is fragmented by nitrogen, forming mixed halide ion complexes, while isobutane transforms mercury halides primarily into an ion complex with a fragment from isobutane (m/z=26). HgBr₂ forms [HgBr₂Cl]⁻ with residual Cl⁻ from previous HgCl₂ runs.

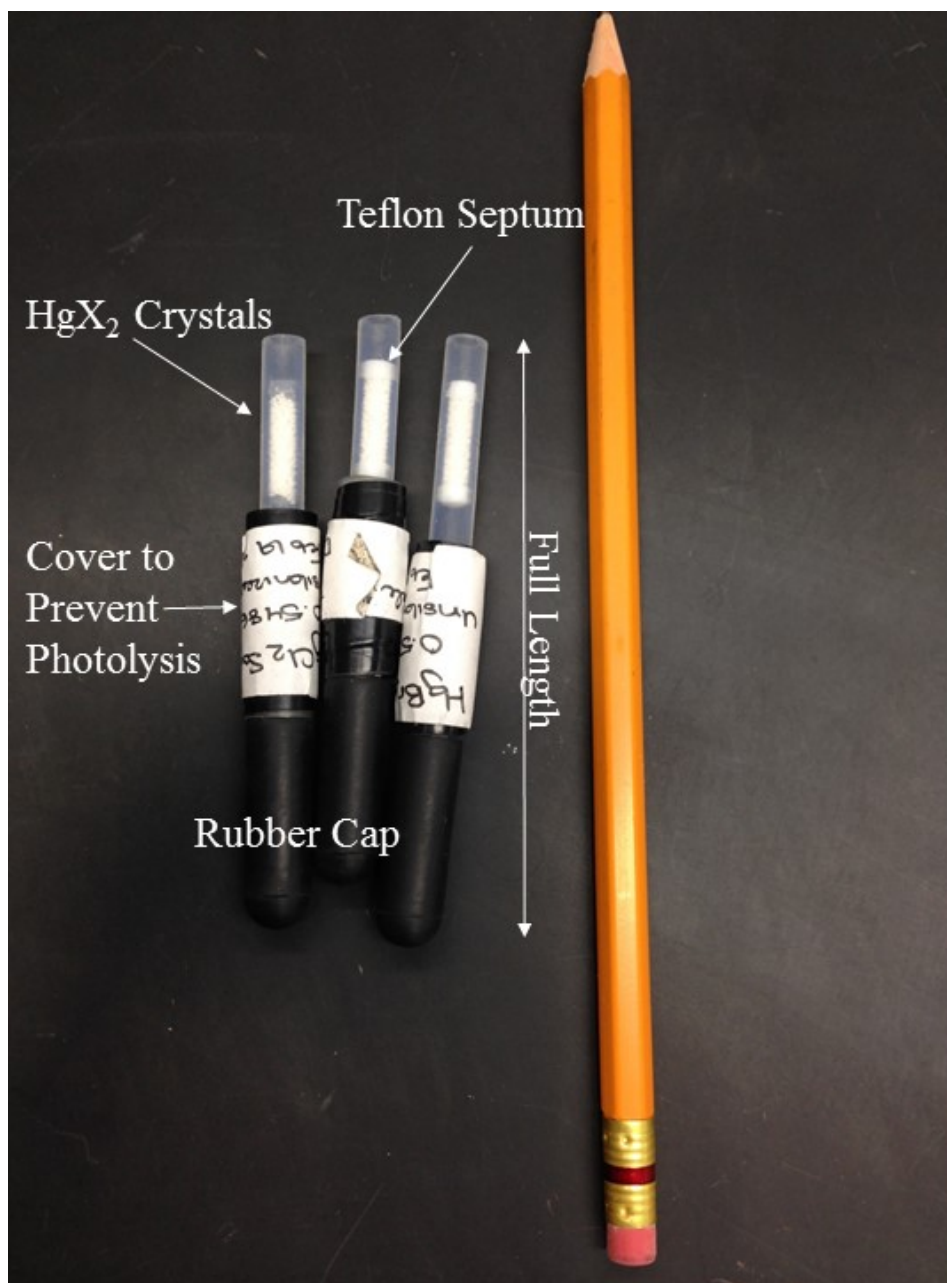


Figure S4 Photograph of mercury halide packed standards, with no. 2 pencil as size reference. The standard consists of a roughly 10 cm length of 6.3 mm ID PFA tubing containing approximately 5 g of mercury chloride, mercury bromide, or a 50:50 HgCl₂:HgBr₂ blend, held in place by either glass wool or Teflon septa. The section of tubing containing HgX₂ is covered to prevent potential photolysis, and the standard is capped by rubber caps, when not in use. This pencil was 18.9 cm long from eraser end to pencil tip

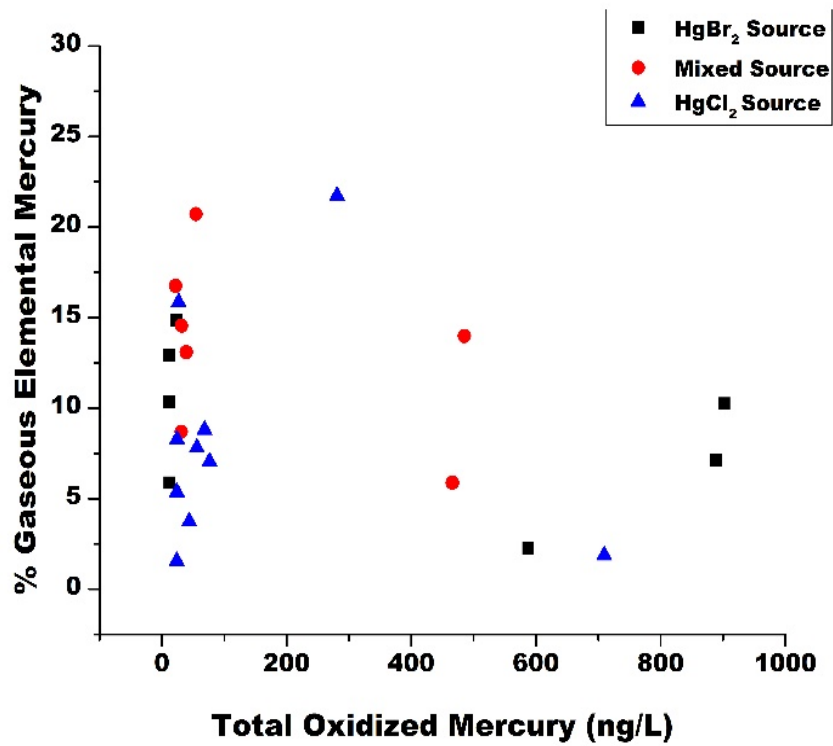


Figure S5 Denuder breakthrough for single and mixed HgX₂ standards at varying Hg(II) concentrations.

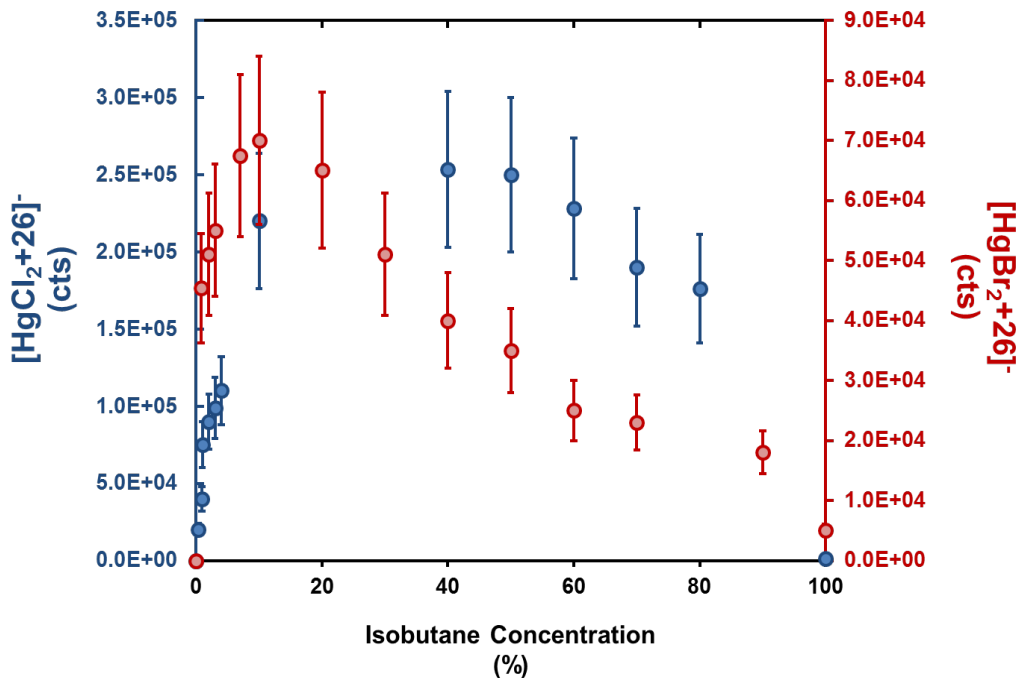


Figure S6 Principal ion signal ($[M+26]^-$, cts) for APCI-MS analyses of HgCl_2 - and HgBr_2 -saturated gas streams with varying concentrations of isobutane in nitrogen. The yield of $[M+26]^-$ increases with increasing isobutane concentrations up to 10-40% isobutane, due to a shift from direct ionization of HgX_2 (and fragmentation) by nitrogen to indirect ionization through isobutane. Increasing isobutane concentrations further reduces $[M+26]^-$ yields, highlighting the role nitrogen plays in producing isobutane ion fragments ($M=26$, presumably C_2H_2^-) for complexation with HgX_2 .

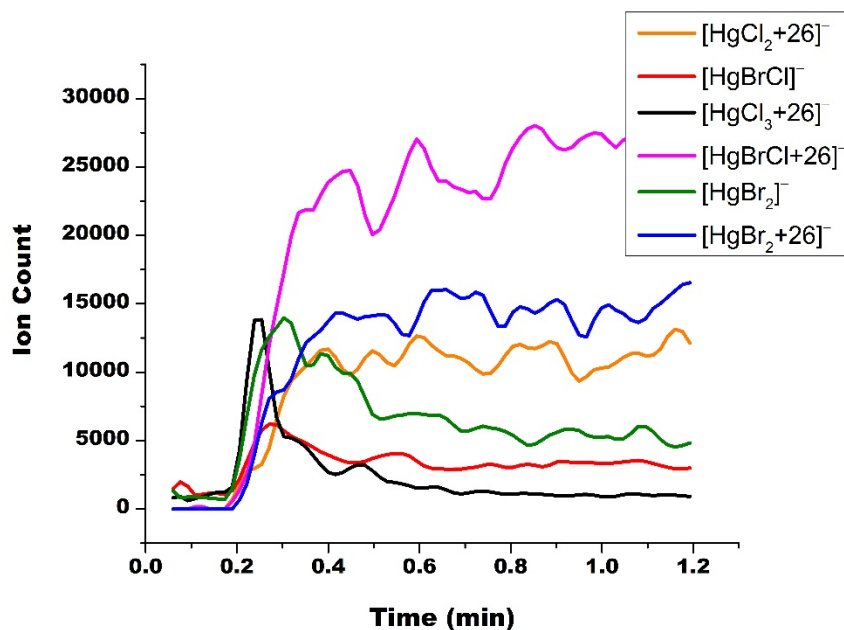


Figure S7 Time evolution of the APCI signal for HgCl_2 and HgBr_2 ions formed using a 10% isobutane in nitrogen CI gas. HgX_2 was collected for 1 min onto a shredded Teflon trap prior to desorption into the APCI inlet at 200°C . The formation of $[\text{HgBrCl}]^-$ (red line) and $[\text{HgBrCl}+26]^-$ (pink line) occurs after both HgCl_2 (as $[\text{HgCl}_3+26]^-$, black line) and $[\text{HgBr}_2]^-$ (green line) ions are present in the APCI inlet.

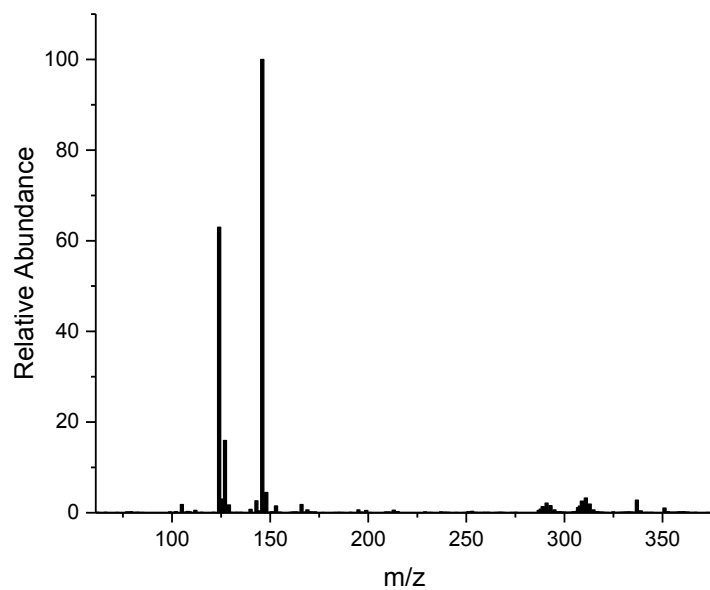


Figure S8 Scan mode (m/z 50 – 400) of 0.5% sulfur hexafluoride in isobutane. Principal ions formed (probable ion in brackets) are $m/z = 147$ ($[\text{SF}_6\text{H}]^-$), 124 ($[\text{SF}_4\text{O}]^-$) and 127 ($[\text{SF}_5]^-$).

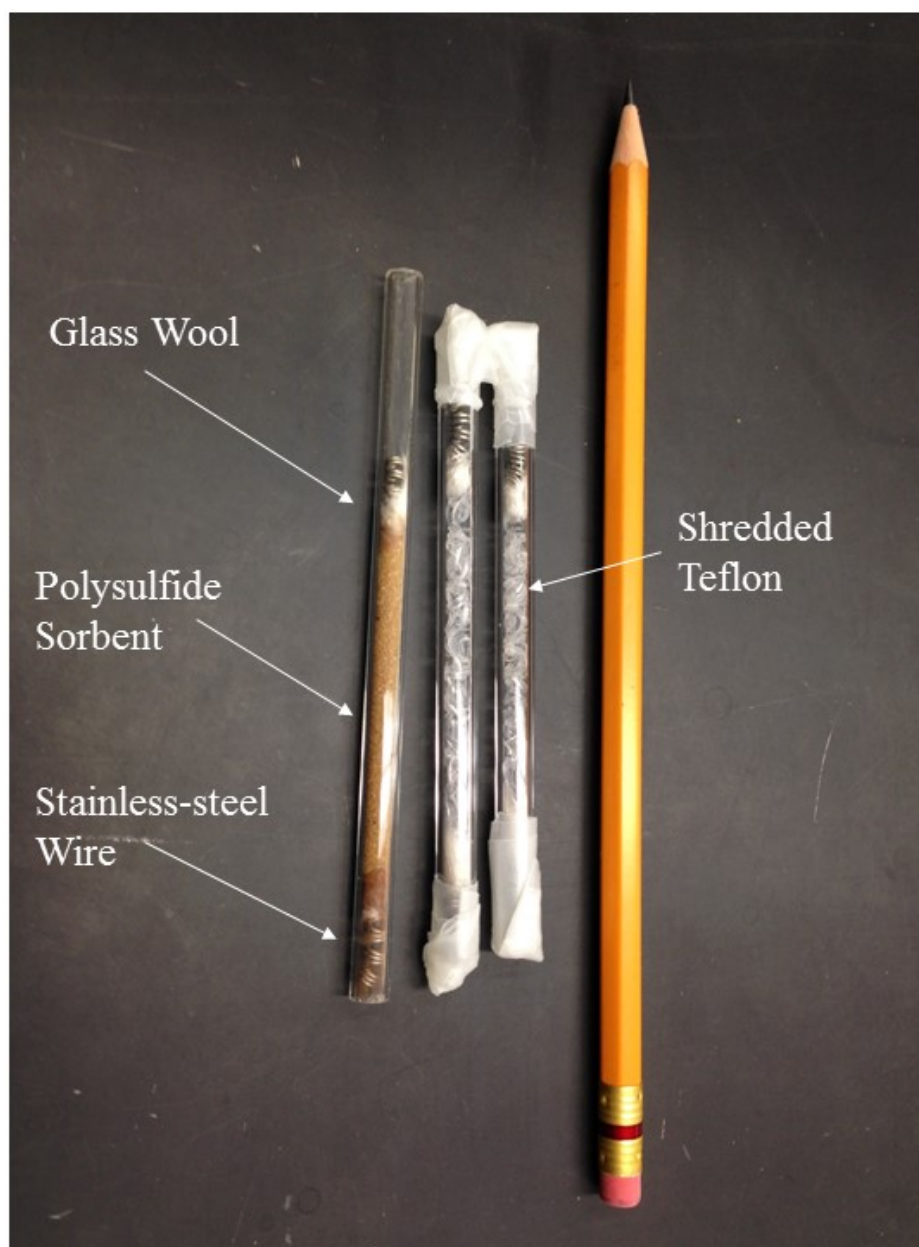


Figure S9 Photograph of polysulfide and teflon sorbent traps used in this study. Sorbent is held in place with glass wool and stainless-steel wire, and capped with paraffin film when stored. This pencil was 18.9 cm long from eraser end to pencil tip

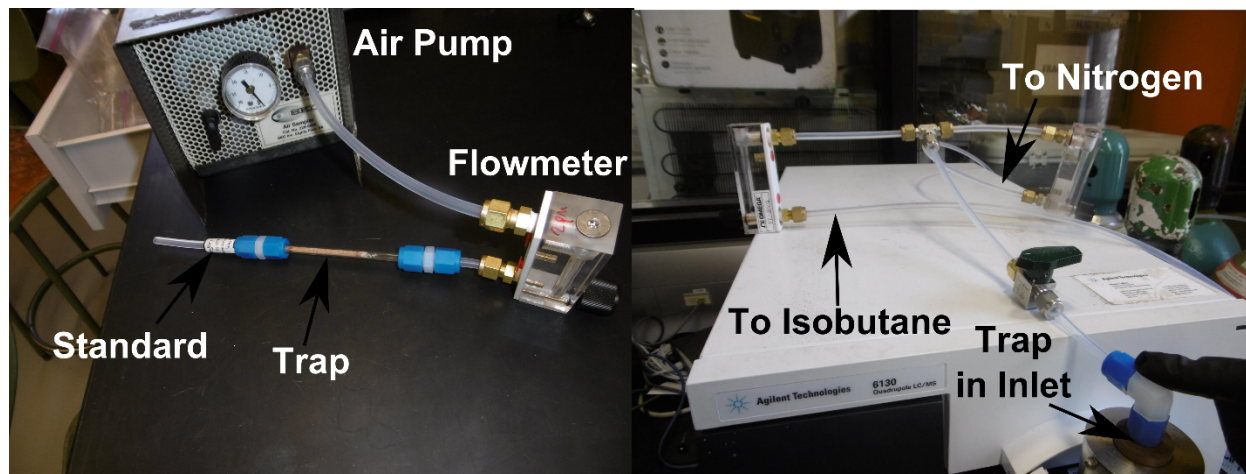


Figure S10 Photographs showing HgX₂ collection (left-hand side) and desorption into APCI inlet (right-hand side). The nitrogen gas line could be reconnected to a sulfur hexafluoride tank when necessary.

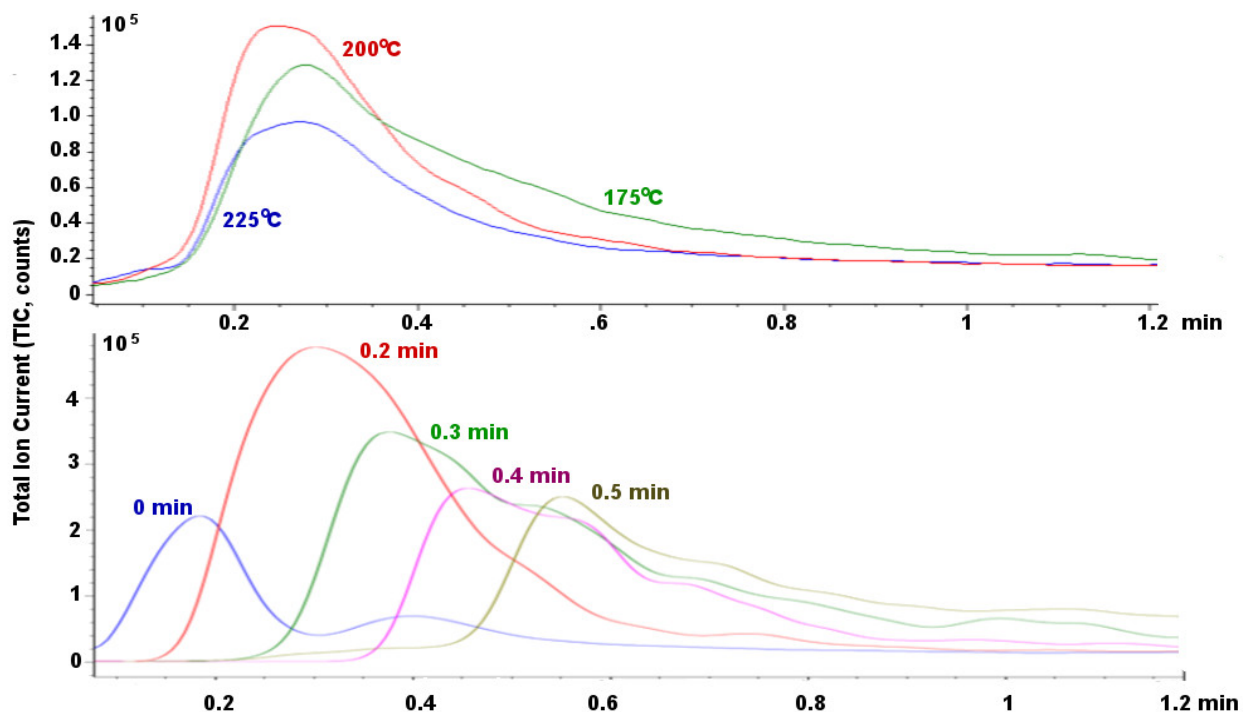


Figure S11 Total Ion Current (TIC) for IB:N₂ APCI detection of HgCl₂ desorbed from a polysulfide trap exposed to a packed HgCl₂ standard over 1 minute at 1 L min⁻¹. Each TIC signal represents the desorption curve of one HgCl₂ collection. The upper plot shows TIC signal for varying inlet temperatures. The lower plot shows TIC as a function of delay between trap insertion and start of CI gas flow (i.e. length of heating period). Heating traps at 200°C for a period of 0.2 min (12 sec) before CI gas flow produced the most well-defined desorption peak.

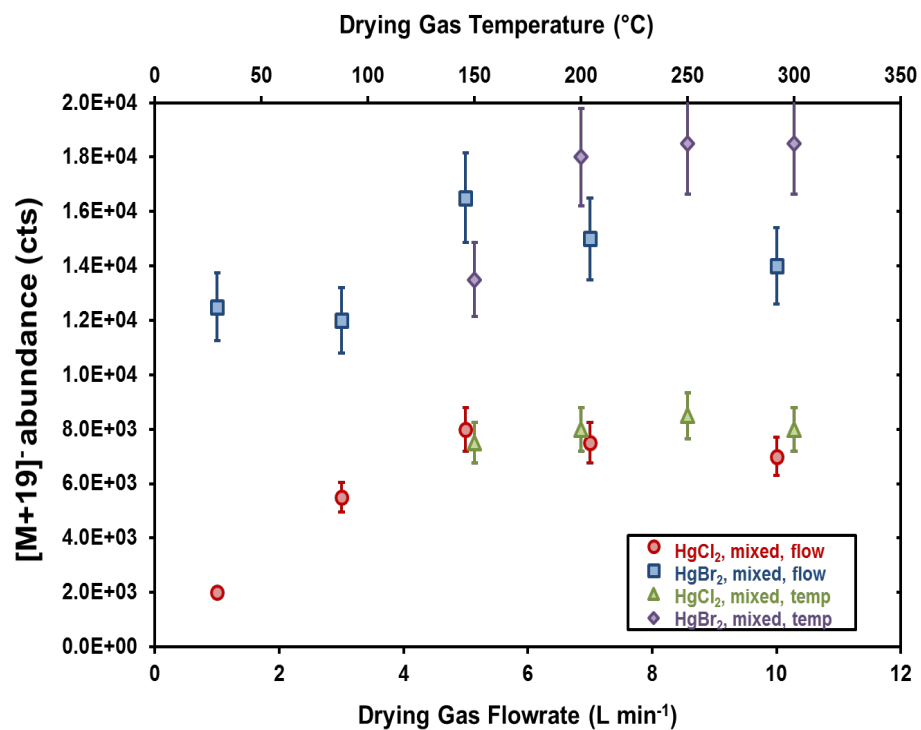


Figure S12 The APCI-MS response to HgCl₂ and HgBr₂ from the mixed HgX₂ standard with varying drying gas flow rate and temperature for HgCl₂ and HgBr₂ using the 0.5% SF₆ in IB blend CI gas. Values are the mean of 3 measurements, with standard deviations of ± 20%. Drying gas temperature for flow tests was 200°C, and drying gas flow rate for temperature tests was 5 L min⁻¹.

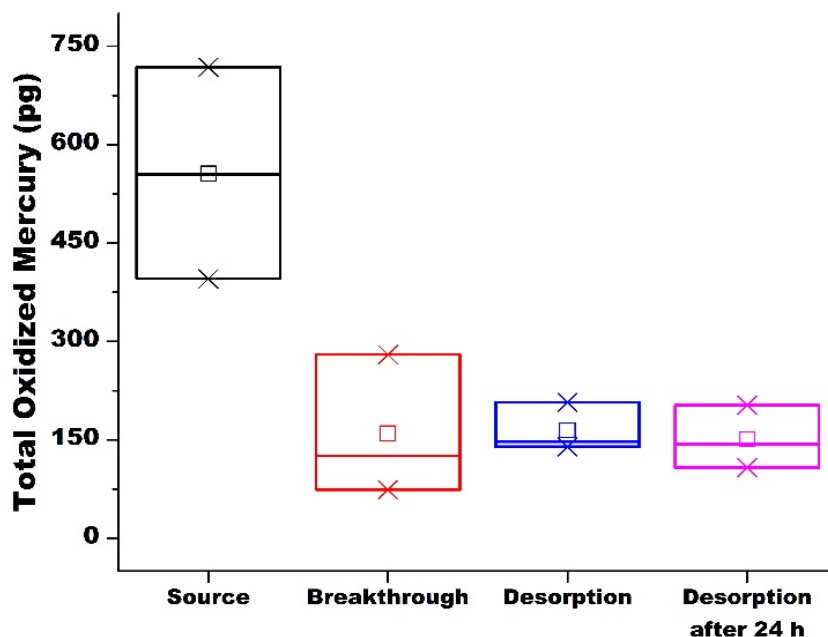


Figure S13 Total Oxidized Mercury (TOM) generated from a mixed $\text{HgCl}_2/\text{HgBr}_2$ source (“Source”) and TOM passing through a Teflon Trap to a KCl denuder downstream (“Breakthrough”). TOM that was collected on the Teflon trap was desorbed at 200 °C for 1 minute into a KCl denuder (“Desorption”). Finally, TOM was measured from a desorption of HgCl_2 and HgBr_2 loaded onto a Teflon Trap after 24 hours of N_2 flow at 1 L min^{-1} through the trap (“Desorption after 24h”). At the 0.05 level, the population mean of Hg^0 vapour (from TOM thermal decomposition) not trapped on a Teflon Trap (“Breakthrough”) is significantly lower ($n=3$, $p=0.0044$) than the TOM generated by the source ($n=3$). The average amount of breakthrough is $28\pm 15\%$. At the 0.05 level, the population mean of Hg^0 vapour (from TOM thermal decomposition) from desorption immediately after loading versus desorption allowing 24 h pumping of N_2 through the trap at 1 L min^{-1} was not significantly different ($n=3$, $p=0.21$).

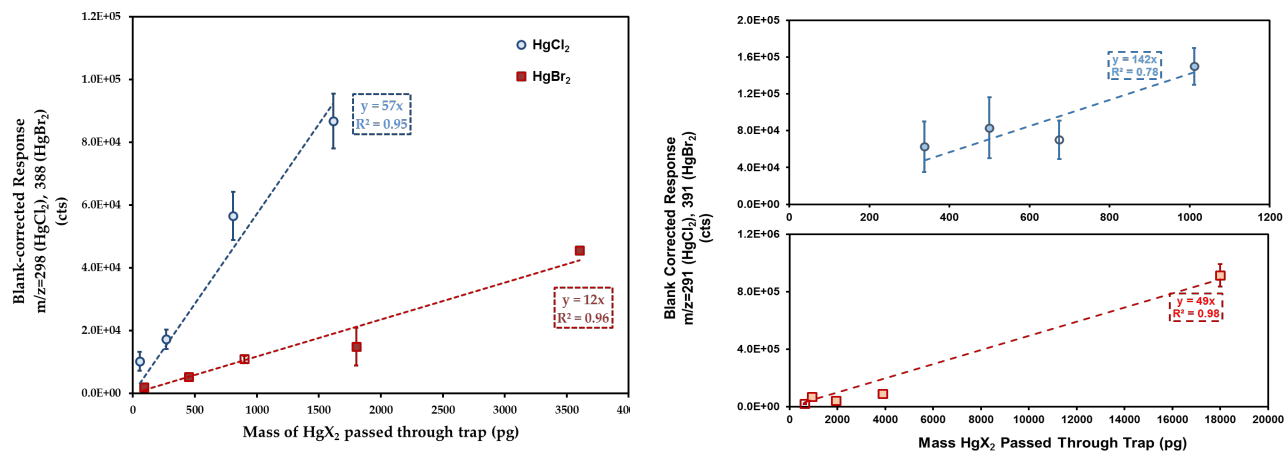


Figure S14 A multi-point calibration of APCI-MS analysis of HgCl₂ (blue circles) and HgBr₂ (red squares) using the PS:IB (left-hand figure) and PFA:SF₆ techniques (right-hand figures). Each point represents the mean 3 measurements (empty symbols 2 measurements), with whiskers indicating 1 standard deviation from the mean.

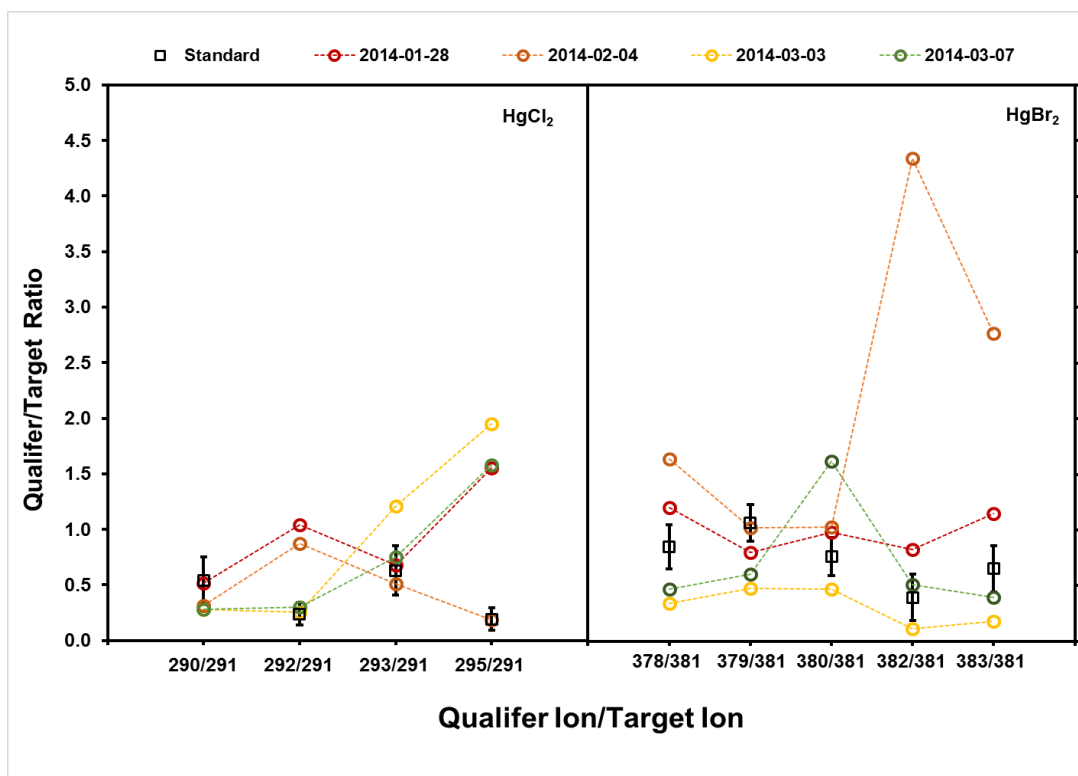


Figure S15 Qualifier/Target (Q/T) ion ratios for SIM mode analyses of HgCl_2 and HgBr_2 in pool air from January to March 2014. HgX_2 standard Q/T ratios are shown in black with whiskers equal to 2 times their standard deviation. Sample Q/T ratios falling within the range indicated by whiskers indicate a positive match with standard Q/T ratios.

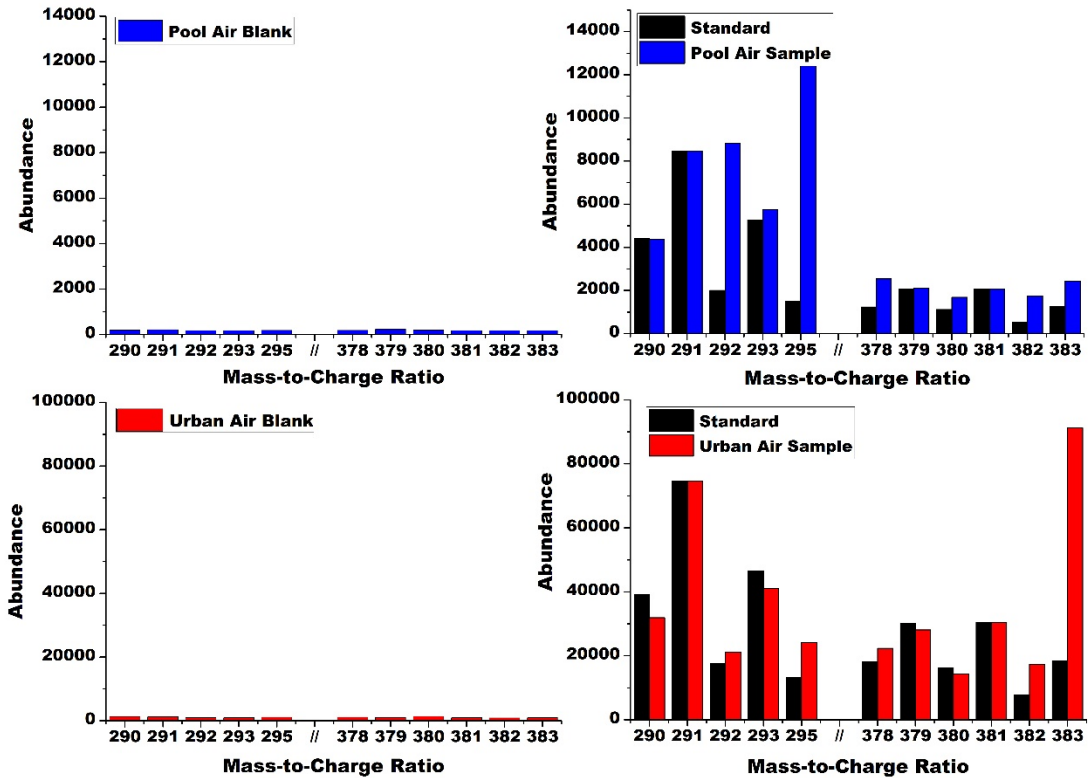


Figure S16 Representative SIM-mode mass spectra for indoor pool air and urban air runs in Montreal, Quebec. Trap blanks (left-hand plots) are negligible compared to air measurements. A SIM-mode spectrum for a 50:50 HgCl_2 : HgBr_2 source is presented for comparison.

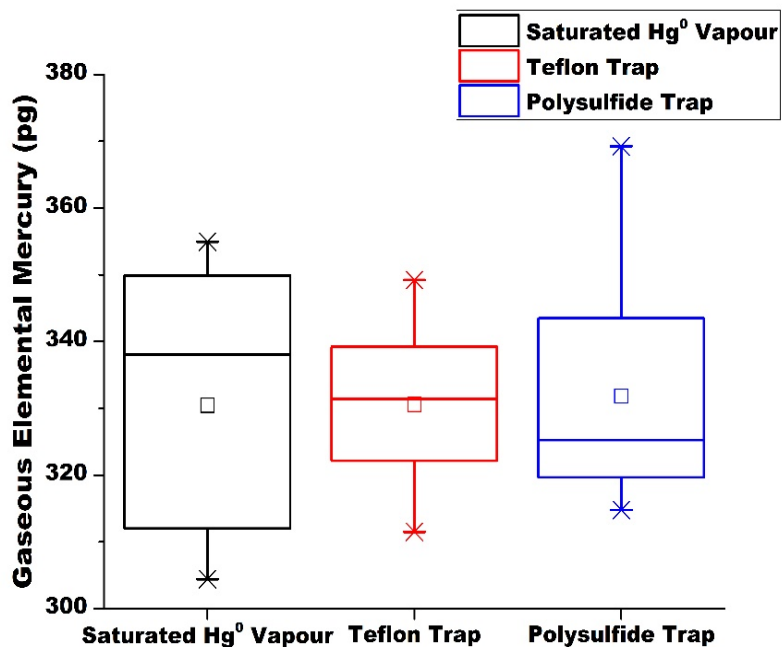


Figure S17 Collection of Hg⁰ vapor on Teflon and Polysulfide (PS) Trap. At the 0.05 level, the population mean of Hg⁰ vapour injected through a Teflon Trap (n=7, p = 0.988) or the PS Trap (n=7, p=0.894) are NOT significantly different from the mean of a direct injection (n=7).